Light Metals 2012 *Edited by: Carlos E. Suarez*
TMS (The Minerals, Metals & Materials Society), 2012

ANALYSIS OF POROUS STRUCTURES OF GRAPHITIC CATHODE MATERIALS AND THE CORRELATION TO PENETRATED SODIUM

Xiang Li, Jilai Xue, Jun Zhu, Qingcheng Zhang
School of Metallurgical and Ecological Engineering, University of Science and Technology Beijing;
Xueyuan Road 30; Beijing 100083, China

Keywords: Cathode, Porous Structure, Image Analysis, Sodium Penetration, Ultrasound

Abstract

Cathode materials used in aluminum reduction cell today are of porous structure. This work is aimed to have better control of the cathode quality through quantitatively analyzing the pore structure and its correlation to the penetrated sodium (metallic Na and NaF). The cathode samples were made of graphite aggregate and pitch, and formed with various pressures (12 – 36 MPa). Image analysis was applied to characterize their porous structures. XRD and SEM-EDS were used to analyze the penetrated sodium in the cathode samples. When the forming pressure was 20 MPa, the cathode density got to its maximum value (1.58 g/cm^3) with the minimum total porosity (21.96 %) and the least pore number (549). When the forming pressure rose from 12 MPa to 36 MPa, the pore connectivity was from 9.81 % up to 37.95 % while the shape factor increased from 1.98 to 2.21 and the depth of sodium penetration became longer from 6 mm to 30 mm. In addition, ultrasound applied can reduce the penetrated sodium in the cathode.

Introduction

Carbon cathodes currently used for aluminum reduction cells have a porous structure. During aluminum electrolysis, the electrolytic melt and sodium penetration as well as carbide formation and dissolution are widely considered as the major causes for cathode deterioration [1], in which the porous structure may play an importance role. The graphitized cathode has excellent resistance to sodium attack, but high production cost and less wear-resistance. The graphitic cathode has higher strength, better wear-resistance, lower price, but worse resistance to sodium attack. However, there is a potential for the graphitic cathode to improve its resistance to bath and sodium penetration, and one of approaches is to have better control of the porous structure of the cathodes.

Several authors have published their work on relationship between porosity and bath penetration. Frolov et al [2] found that the bath penetration depth depended on open porosity. Brisson et al [3] showed that the metallic sodium in semi-graphitic blocks was presented in microspores or intercalated within the graphene layers. In graphitic blocks, however, the metallic sodium was only detected in the microspores. In the work of El-Raghy et al [4-5], the porosity of cathode was decreased from 15 % to 1.5 % by impregnation of a high carbon yield resin (furfuryl alcohol), thus reducing Na penetration about 65 % compared with the untreated carbon block.

In previous work, the correlation between the sodium penetration and the porous structures of three industrial cathode materials (semi-graphitic, graphitic and graphitized cathodes) has been investigated extensively [6-7]. The semi-graphitic cathode was found having a higher total porosity, in which the pores were aligned in certain directions causing a higher connectivity that could facilitate to sodium and cryolite penetration into the cathode. The graphitic cathode had lower total porosity and connectivity, which could contribute to a lowered sodium penetration. And the graphitized cathode showed the best resistance to the sodium attack, which was due to its lower connectivity besides the high degree in graphitization. These findings above are considered as compelling reasons that a better control of the porous structures of cathodes can improve the resistance to the bath and sodium penetration. However, the mechanism of the porous structures correlated with such penetration remains unclear. Furthermore, a better quantitative approach charactering the structure features of the cathode materials associated with the bath and sodium penetration is needed for both the scientific and practical purposes.

In this paper, graphitic cathodes samples were made in laboratory and characterized using Image Analysis. And the bath and sodium penetration experiments were carried out in a laboratory aluminum electrolysis cell with rotating electrode method. XRD and SEM-EDS were used to analyze the penetrated sodium in the cathode samples. This work could offer theoretical support to further control the structures of cathode pores. In addition, this paper originally investigated the effects of ultrasound on the bath penetration into the cathode during aluminum electrolysis.

Experimental

Preparation of Cathode Samples

Figure 1 is the flowing chart of preparing graphitic cathode samples. Graphite particles with varied granularity were mixed with a constant amount of medium hard pitch in a mixing machine at 140 °C. And then the green samples were formed at a pressure varied from 12 MPa to 36 MPa. They were baked at 1200 °C in a vessel packed with fresh carbonaceous powders. The testing samples were in cylindrical form with a dimension of 25 mm diam × 60 mm length.

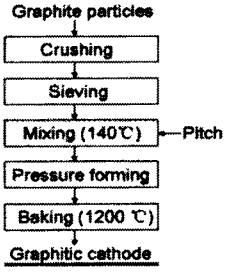

Figure 1. Flowing chart of preparing graphitic cathode samples.

Various physical properties were examined, including apparent density by measuring their weight and geometric dimensions, open porosity by the hydrostatic method (National Standard, GB6156), electrical resistance at room temperature by the 4-terminal method (National Standard, GB6717), and air permeability by gas permeameter.

Image Analysis

The test specimen for inspecting was sectioned from the cathode sample, perpendicular to its longitudinal axis. Then the half of the specimen was embedded in epoxy by vacuum casting equipment. The cross section that had been ground and polished was examined by a standard polarization microscope (Leica, DMRX). Five arbitrary regions (768×582) were captured on each sample. Image analysis software (Image J) was used for processing the photographs and charactering the porous structures of the cathode samples, as described previously [7].

Sodium Penetration

Figure 2 shows the experimental set-up for sodium penetration during aluminum electrolysis. The electrolysis cell was placed in a vertical tube furnace. The sodium penetration experiments were carried out with rotating cathode. During the electrolysis, the cylindrical cathodes were immersed 2 mm in the cryolitic melts and rotated at a speed of 120 r.p.m for maintaining a uniform mass transportation. The test temperature was 960 °C, and the current density at cathode was 0.5 A/cm^2 constantly. The whole process was operated under argon atmosphere.

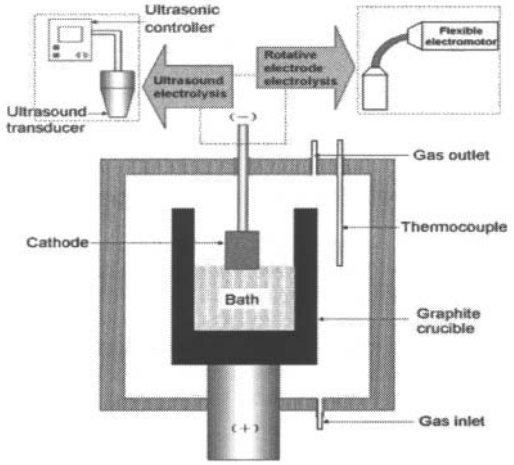

Figure 2. Schematic drawing of sodium penetration experiment with an ultrasonic system.

Ultrasound was introduced through the cathode rod that was placed in the electrolysis cell. The sonic waves with a frequency of 20 kHz were transferred into the interface of the cathode and the melt. The power of ultrasound was 540 W and loaded into the cathode for 2 seconds and stopped off for 2 seconds, alternatively.

The chemicals used in the experiment are shown in Table I. The electrolytic bath that all test used was prepared before each experiment. The different masses of chemicals were calculated to obtain the required cryolite ratio (CR) of 2.5 (mol NaF/ mol AlF_3) with 8 % Al_2O_3 and 5 % CaF_2.

Table I. Materials and Chemicals Used in Experiments

Materials	Specifications
Na_3AlF_6-AlF_3	Technical grade, CR = 2.0
NaF	Purity: ≥ 99.99 wt.%
Al_2O_3	Purity: ≥ 99.0 wt.%
CaF_2	Purity: ≥ 98.5 wt.%

Phenolphthalein Test and SEM-EDS Characterization

The sodium penetrated samples were cut off along the longitudinal axis, and one section was in contact with a liquid layer of phenolphthalein in a glass dish. Then the surface of the cross-section was pressed against a filter paper. If metallic sodium is at present, a red-color area will appear on the filter paper, indicating the sodium penetration depth within the sample.

Another section was examined by SEM-EDS micro-area techniques with scanning time of 90 seconds crossing the area for each 1 mm along the axis direction, as described previously [6]. The penetrated melts in the cathode samples were then expressed against the penetration depth.

Results and Discussion

Physical Properties of Cathode Samples

In Table II, the physical properties of tested cathode samples are shown. When the forming pressure was changed from 12 MPa to 36 MPa, there were small changes in both cathode density and open porosity. But when the pressure was increased to 36 MPa, the values of resistivity at room temperature and the air permeability obviously increased.

Table II. Physical Properties of the Cathode Samples

Samples No.	Forming pressure (MPa)	Apparent density (g/cm^3)	Volume expansibility (%)	Mass loss rate (%)	Open porosity (%)	Resistivity 20 °C (μΩ·m)	Air permeability (10^{-3}μm^2)
12B	12	1.55	5.02	-8.92	23.33	29.30	101.0
20B	20	1.58	4.05	-8.55	22.19	29.42	89.7
28B	28	1.56	6.18	-8.62	23.02	28.78	86.2
36B	36	1.55	9.13	-7.60	22.02	34.60	615.0

The air permeability reflects the ability of gas going through the inner area of the sample with a defined cross-section, thickness, pressure and time. It is related to the density, porosity, pores diameter and pores connectivity. The air permeability for sample 36B is the highest in value, and it means that the sample usually has higher pore connectivity.

With increasing the forming pressure from 12 MPa to 20 MPa, the graphitic particles could be pressed together, thus limiting the pitch binder from volatilization and increase the amount of carbon residue. This made an increase in density (sample 20B). However, with further increasing the forming pressure up to 36 MPa, the physical property for the sample 36B varied in association with volume expansion and mass loss, which could be due to an over-pressured forming. This may result in grains crash and micro-cracks within the cathode samples, and induce a porous structure increasing the air permeability and the electrical resistivity.

Characterization of Porous Structures

Figure 3 shows the grayscale and binary pores images for four cathode samples. Porous structures of cathodes were analyzed by image analysis technique.

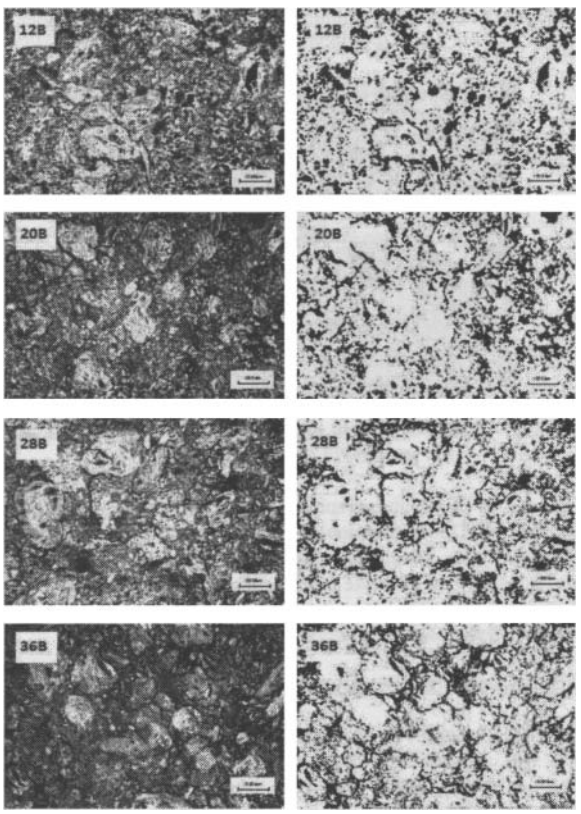

Figure 3. Grayscale and binary pores images for cathode samples. (Grayscale images on the left and binary images on the right)

In Table III, the statistical results of image analysis on the pores, where several parameters have been selected to characterize the pores in the cathode samples statistically, as follows:

1. Total porosity: the ratio of pores area to the total inspected area.
2. Pore numbers: an average data on five inspected regions (768×582), ignoring pores smaller than 10μm (in diameter).
3. Aspect ratio: ratio between major diameter and minor diameter of an equivalent ellipse to the object (a pore).
4. Connectivity: percentage of connecting lines' length to the total objects' length in Skeletonization, where the connecting line was defined to the skeleton line longer than 3 mm.

Table III. Statistical Results of Image Analysis on the Pores in Cathode Samples

Samples	Total porosity (%)	Pore numbers	Aspect ratio	Connectivity (%)
12B	22.56	685	1.98	9.81
20B	21.96	549	2.11	14.20
28B	22.04	601	2.12	20.49
36B	23.46	579	2.21	37.95

When the forming pressure was 12 MPa, the sample exhibited a higher total porosity (22.56 %), highest number of pores (685) and lowest aspect ratio (1.98). The shapes of most pores in 12B were close to circle. When the pressure increased, pore numbers decreased, while the aspect ratio and connectivity of the pores became higher. The pores on sample 36B had the highest aspect ratio (2.21) and connectivity (37.95 %). It means that high pressure made the pores elongated and connected.

Analysis of Penetrated Sodium

Figure 4 shows the XRD results of sample 20B before and after the aluminum electrolysis. The other samples compositions are similar. After electrolysis, the phases found in the cathode samples were most graphite and NaF. It indicates that NaF was the main melt compound into the cathodes.

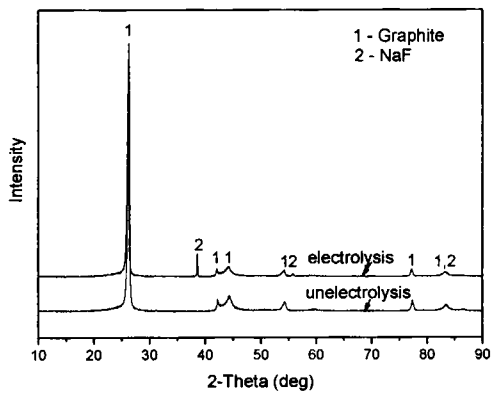

Figure 4. XRD results of sample 20B before and after aluminum electrolysis (CD= 0.5 A/cm^2, 960 °C).

Haupin [8] and Thonstad [9] have argued that metallic aluminum is probably generated by the reactions:

$$AlF_4^- + 3e^- \rightarrow Al(l) + 4F^-(melt) \quad (1)$$

$$[Al_2OF_6]^{2-}(melt) + 3e^- \rightarrow Al(l) + [AlOF_2]^-(melt) + 4F^-(melt) \quad (2)$$

No matter which reaction occurs, Al^{3-} must diffuse into the boundary layer of cathode, and corresponding Na^+ must be accompanied in order to keep electric neutrality. When the Al^{3-} turns to metallic aluminum, generated F^- is combined with Na^+ and turns into NaF.

$$4F^-(melt) + 4Na^+(melt) \rightarrow 4NaF(melt) \quad (3)$$

It made that NaF enriches near the cathode surface, which elevate the liguidus temperature and worsen the liquidity of the melts. Even though flexible electromotor was used, it was hard for generated NaF to diffuse or flow to the bulk melts. Most NaF penetrated into the cathode with capillary force.

Figure 5 shows the results of phenolphthalein test. No phenolphthalein color lightered on sample 12B. The coloration depths of 20B and 28B were close (about 8~10 mm), but the color of 20B was lighter than 28B. The coloration depth of 36B was 17 mm. It means there was no or very little metallic sodium in the sample 12B, but there was the most metallic sodium penetration into the sample 36B.

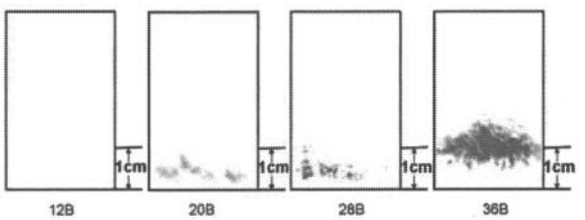

Figure 5. Results of phenolphthalein test (CD= 0.5 A/cm^2, 960 °C).

The starting position of phenolphthalein color had a certain distance from the bottom. This phenomenon was the most obvious in sample 36B. The color starting position of 36B was about 6mm from the bottom. Brilloit et al [10] used to call this no color area as "white band". They thought that penetrated metallic sodium had reacted with electrolyte in this area, as equation (4) shown.

$$4Na_3AlF_6(l, in\ C) + 12Na(g, in\ C) + 3C(s) \rightarrow Al_4C_3(s, in\ C) + 24NaF(l, in\ C) \quad (4)$$

At 960 °C, ΔG^0 = -266.377 kJ/mol for reaction (4). Na_3AlF_6 reacted with the penetrated metallic sodium, which consumed inner metallic sodium and generated NaF. With more Na_3AlF_6 penetration, "White band" area was larger. And this is another reason that the penetrated phase found in the cathode samples was most NaF.

Phenolphthalein test is simple and convenient, but parts of metallic sodium reacted makes the phenolphthalein test results inaccurate. Because generated sodium element exist all the time, total sodium in the cathode can reflect the depth and amount of sodium penetration. Accordingly, SEM-EDS micro-area analysis was used to determine the depth and amount of penetrated total sodium.

Figure 6 shows SEM-EDS examination results. It can be seen that the sodium can continuously migrate into the carbon cathodes. The percentage of penetrated sodium, which could include metallic Na, NaF and Na_3AlF_6, increased in the order of 36B≫ 28B≈20B>12B. It was similar to phenolphthalein tests.

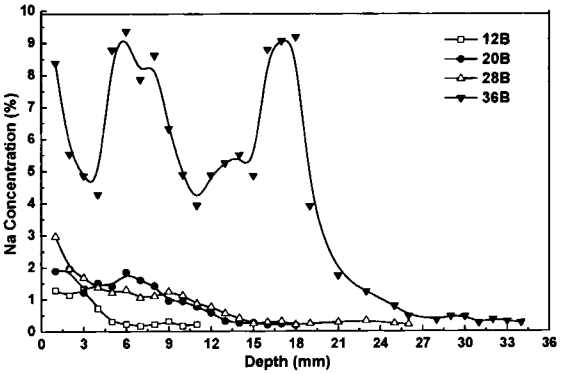

Figure 6. Penetrated sodium *vs.* penetration depth in cathode samples after aluminum electrolysis.

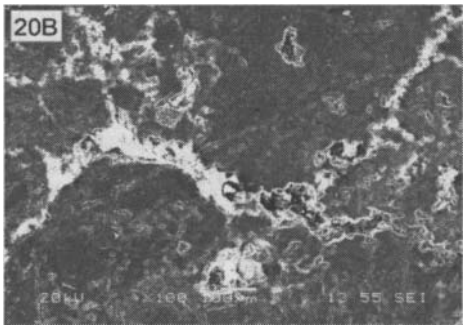

Figure 7. SEM micrograph showing the cross-section of cathode sample 20B after electrolysis.

Figure 7 is SEM micrograph of sample 20B cross-section after electrolysis. The other samples' micrographs are quite similar to this one. The penetrated electrolytes existed in the micro-structures formed after the binder volatilizing and carbonizing. It is surmised that this micro-pores played an important role in the bath penetration during aluminum electrolysis.

Correlation of Porous Structures with Penetrated Na and F

From the results of Image Analysis, it is found that the sample 36B had the minimum pore numbers and pores were mostly elongate shape, which caused its aspect ratio and connectivity highest in the samples. And it is observed that the melt cryolite penetrated into the cathode among the pores and micro-cracks. When the aspect ratio and connectivity were high, the sodium and cryolite penetrated into cathode more easily, so the sample 36B exhibited the worst resistance to bath penetration. Although there was the maximum pores number of sample 12B, the shapes of the pores were closer to circle (aspect ratio closer to 1) with the

minimum connectivity. It means most of the pores were independence, and the bath penetrated into the cathode hardly. Thus, the sample 12B had the lowest bath penetration. For the sample 20B and 28B, the parameters of the pore structure were consistent approximately, which made the similar bath penetration.

Na_3AlF_6 reacted with the penetrated metallic sodium, which destroyed the matrix of carbon and made the sodium penetration easier. More penetrated Na_3AlF_6 caused the element sodium increasing in cathode by promoting the metallic sodium and NaF generation. By improving the pore structures, such as making the pore independence with close circle shape, and deducing the elongated and connected pores, it can prevent the sodium related with Na_3AlF_6 penetration into the cathode.

Effects of Ultrasound on Bath Penetration into Cathodes

Figure 8 shows the phenolphthalein test results of the cathode after electrolysis. Obviously, when ultrasound was applied on the cathode samples, the penetrated sodium was lowered than the samples without ultrasound. And the effect of ultrasound on restricting the sodium penetration was more evident under lower current density.

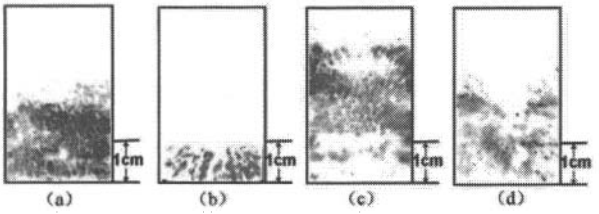

Figure 8. The results of phenolphthalein test (a= 0.5 A/cm^2, no ultrasound; b= 0.5 A/cm^2, on ultrasound; c= 1 A/cm^2, no ultrasound; d= 1 A/cm^2, on ultrasound. All samples without rotation).

Figure 9 shows the information of the cathode bottom after electrolysis (CD = 1.0 A/cm^2) with ultrasound -off and -on. With ultrasound-off, there was solidified cryolite on the cathode bottom, as Figure 9(a) shown. The aluminum produced was dispersed in the bath. But when the ultrasound was applied on the cathode, it was found that the aluminum produced was adhered to the cathode bottom uniformly, as Figure 9(b) shown. It means that the melt Al wetting on the cathode was changed with ultrasound -on.

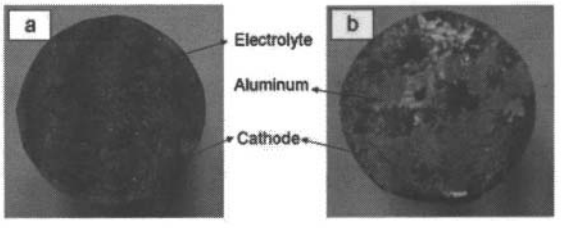

Figure 9. The photograph of cathode surface in contact with melt (a is the sample after normal electrolysis; b is the sample after ultrasound electrolysis).

Xue and Oye [11] have found the cell voltage can be dropt when ultrasound was applied on the anode during aluminum electrolysis. And in the previous work, it has been found that the dissolution behavior of melt Al in the cryolite was changed with ultrasound [12]. But the mechanism of ultrasound effects on cathode is not clear. The more details will be investigated on the mechanism of ultrasound effect on the wettability and penetration.

Conclusions

1. The forming pressure in lower range has little effect on the apparent density and open porosity for the graphitic cathode samples, while a higher forming pressure can increase the room temperature resistivity and the air permeability.

2. Image Analysis indicates that a higher forming pressure can decrease the pore numbers while increase the aspect ratio and connectivity due to the pores elongated and connected, and again enhance the cryolite and sodium penetration into the cathode body.

3. NaF is the major phase penetrated into cathode after aluminum electrolysis, which are partly from the reaction of Na_3AlF_6 with the penetrated metallic sodium in carbon and such a reaction further makes sodium penetration easier due to the damage of the carbon matrix; improving the pore structures can prevent the sodium related with Na_3AlF_6 penetration into the cathode.

4. When ultrasound is applied on the cathode during the aluminum electrolysis, the penetrated sodium in the cathodes is reduced.

Acknowledgement

Part of work has been supported by National Natural Science Foundation of China (No. 50874012).

References

1. L.P. Lossius and H.A. Øye, "Melt Penetration and Chemical Reactions in 16 Industrial Aluminum Carbon Cathodes," *Metallurgical and Materials Transactions B*, 31B (12) (2000), 1213-1224.

2. A.V. Frolov et al., "Wetting and Cryolite Bath Penetration Graphitized Cathode Materials," *Light Metals 2006*, 2006, 645-649.

3. P.Y. Brisson et al., "X-ray Potoelectron Spectroscopy Study of Sodium Reactions in Carbon Cathode Blocks of Aluminium Oxide Reduction Cells," *Carbon*, 44 (1) (2006), 1438-1447.

4. S.M. El-Raghy et al., "Porosity Modifications in the Carbon Cathode of Aluminum Reduction Cell," *Light Metals 2001*, 2001, 723-729.

5. S.M. El-Raghy, F.M. Ahmed, and M.O. Ibrahiem, "Porosity Modifications in the Carbon Cathode of Aluminum Reduction Cell –II," *Light Metals 2002*, 2002, 63-69.

6. J. Xue et al., "Characterization of Sodium and Bath Penetration in Industrial Graphitic and Graphitized Cathodes," *EPD Congress Volume 2010*, 2010, 591-598.

7. Y. Gao et al., "Characterization of Sodium and Fluoride Penetration into Carbon Cathodes by Image Analysis and SEM-EDS Techniques," *Light Metals 2011*, 2011, 1103-1107.

8. W.E. Haupin, "Principles of Aluminum Electrolysis," *Light Metals 1995*, 1995, 195-203.

9. J. Thonstad et al., *Aluminium Electrolysis-Fundamentals of the Hall-Heroult Process* (Düsseldorf: Aluminium-Verlag, 3rd Ed., 2001).

10. P. Brilloit, L.P. Lossius, and H.A. Øye, "Penetration and Chemical Reactions in Carbon Cathodes during Aluminum Electrolysis: Part I. Laboratory Experiments," *Metallurgical Transactions B*, 24B (2) (1993), 75-89.

11. J. Xue and H.A. Øye, "Bubble Behaviour-Cell Voltage Oscillation during Aluminum Electrolysis and the Effects of Sound and Ultrasound," *Light Metals 1995*, 1995, 265-271.

12. J. Xue et al., "Direct Observation of Al Drop and Gas Bubbles in the Anode-Cathode Space during Aluminum Electrolysis," *EPD Congress Volume 2011*, 2011, 875-881.